

Novel Ferroelectric and Electroclinic Organosiloxane Liquid Crystals

J. Naciri,* J. Ruth, G. Crawford, R. Shashidhar, and B. R. Ratna

Center for Bio/Molecular Science and Engineering, Code 6950, Naval Research Laboratory, Washington DC 20375

Received February 16, 1995. Revised Manuscript Received April 19, 1995*

A new series of organosiloxane ferroelectric liquid crystalline materials have been synthesized, and their mesomorphic and physical properties have been characterized. The new series contains a siloxy chain attached to the hydrocarbon chain at the nonchiral end of the molecule. All materials show a very low melting point ($<5\text{ }^{\circ}\text{C}$) and exhibit chiral smectic A (SmA) and chiral smectic C (SmC*) mesophases. The changes in the siloxy chain length strongly affect the mesomorphic behavior and electrooptic properties of these materials. Increasing the number of siloxy units in the chain increases the temperature range of the SmA phase, with a concomitant decrease in the SmA–SmC* transition temperature. The electroclinic effect in the smectic A phase is characterized by a large electroclinic coefficient ($\sim 4\text{ }^{\circ}\text{V}^{-1}\text{ }\mu\text{m}^{-1}$ at $T-T_{AC^*} = 2\text{ }^{\circ}\text{C}$) and low switching time ($<40\text{ }\mu\text{s}$). One of the materials shows one of the highest value of spontaneous polarization P_s ever reported in the SmC* phase for similar siloxane materials with $P_s = 342\text{ nC cm}^{-2}$ at $25\text{ }^{\circ}\text{C}$.

Introduction

Ferroelectric liquid crystal (FLCs) materials exhibiting room temperature chiral smectic C (SmC*) or chiral smectic A (SmA) phases and low melting temperatures are of great interest in the electrooptic field. They are the basis of a variety of potential devices ranging from large-area flat-panel displays,¹ ultrafast electro-optic modulators,² and spatial light modulators.³ They are also being considered for novel nonlinear optical applications.⁴ Chiral smectic C materials are appropriate for applications where bistability is required, whereas chiral smectic A materials are suited for gray-scale applications.

Typically, FLC molecules consist of a rigid core and end-tail groups with a chiral center located on one or both groups. For most FLC molecules, the end-tail groups are hydrocarbon chains. However, recently there has been some effort to study the effect of replacing the alkyl chains partially with either fluorocarbons⁵ or siloxy units.^{6,7} In contrast to the stiff fluorocarbons, the partial substitution of alkyl chains

by more flexible dimethylsiloxane groups is expected to enhance the thermal stability and lower the phase transition temperatures of the LC materials.⁶ Dimethylsiloxane groups are bulky and more flexible and exhibit more irregular conformations, compared to their alkyl chains counterparts. This has the effect of reducing the shape anisotropy of the molecules and hence its degree of crystallinity. Reduction of crystallinity to below ambient temperatures is of great interest from an application point of view.

This approach of decreasing the crystallinity of mesogens has already been performed in side-chain liquid-crystal polymers.⁸ However, incorporation of siloxy groups in the alkyl chains of FLC low molecular mass has not been well exploited so far. In fact, only a few examples of organosiloxane-related FLC materials have been published.^{6,7} In this paper, we present the synthesis and characterization of new ferroelectric organosiloxane materials which exhibit room temperature chiral smectic C phase and low melting points ($<5\text{ }^{\circ}\text{C}$). We will discuss the influence of the dimethylsiloxane chain length on the mesophase temperatures and electrooptic properties of these materials in detail.

* Abstract published in *Advance ACS Abstracts*, June 1, 1995.

(1) Kanbe, J.; Inoue, H.; Mizutome, A.; Hanyuu, Y.; Katagiri, K.; Yoshihara, S. *Ferroelectrics* **1991**, *114*, 3.

(2) (a) Walba, D. M.; Rego, J. A.; Clark, N. A.; Shao, R. Studies on Ferroelectric Liquid Crystal Tolan Derivatives Designed for Nonlinear Optical Applications. In *Macromolecular Host-Guest Complexes: Optical and Optoelectronics Properties and Applications*; Jenekhe, S. A., Ed.; Materials Research Society: Pittsburgh, PA, 1992; Vol. 277, p 205. (b) Walba, D. M.; Zummach, D. A.; Wand, M. D.; Thurmes, W. N.; Moray, K. M.; Arnett, K. E. Synthesis of Ferroelectrics Liquid Crystal Oligomer Glasses for Second Order Nonlinear Optics. *Liquid Crystal Materials, Devices, and Applications II*, Wand, M. D., Efron, U., Eds.; Proc. SPIE **1993**, *1911*, 21.

(3) Handschy, M. A.; Drabik, T. J.; Cotter, L. K.; Gaalema, S. D. Fast Ferroelectrics-Liquid-Crystal Spatial Light Modulator with Silicon-Integrated-Circuit Active Backplane. *Optical Digital GaAs Technology, Signal Processing Applications*; Proc. SPIE **1990**, *1291*, 158.

(4) (a) Walba, D. M.; Ros, M. B.; Sierra, T.; Rego, J. A.; Clark, N. A.; Shao, R.; Wand, M. D.; Vohra, R. T.; Arnett, K. E.; Velsco, S. P. *Ferroelectrics* **1991**, *121*, 247. (b) Scmitt, K.; Herr, R. P.; Schadt, M.; Fünfschilling, J.; Bucheher, R.; Chen, X. H.; Benecker, C. *Liq. Cryst.* **1993**, *14*, 1735. (c) Sprunt, S.; Naciri, J.; Ratna, B. R.; Shashidhar, R. *Appl. Phys. Lett.* **1995**, *66*, 1443.

Experimental Section

Techniques. The 300 MHz ^1H NMR spectra were recorded on a Bruker MSL300 spectrometer in CDCl_3 or DMSO solu-

(5) Naciri, J.; Crawford, G. P.; Ratna, B. R.; Shashidhar, R. *Ferroelectrics* **1993**, *148*, 297.

(6) Sunohara, K.; Takatoh, K.; Sakamoto, M. *Liq. Cryst.* **1993**, *13*, 283.

(7) (a) Coles, H. J.; Owwen, H.; Newton, J.; Hodge, P. *Liq. Cryst.* **1993**, *15*, 739. (b) Redmond, M.; Coles, H. J.; Wischerhoff, E.; Zentel, R. *Ferroelectrics* **1993**, *148*, 323. (c) Newton, J.; Coles, H.; Owen, H.; Hodge, P. *Ferroelectrics* **1993**, *148*, 379. (d) Newton, J.; Coles, H.; Hodge, P.; Hannington, J. *J. Mater. Chem.* **1994**, *4*, 869.

(8) (a) Naciri, J.; Pfeiffer, S.; Shashidhar, R. *Liq. Cryst.* **1991**, *10*, 585. (b) Naciri, J.; Schnur, J.; Shashidhar, R. US Patent 5,252,695, **1993**. (c) Naciri, J.; Mery, S.; Pfeiffer, S.; Shashidhar, R. *J. S. I. D.* **1994**, *2*, 175.

tions. Infrared spectra were obtained by using a FT Perkin-Elmer 1800 spectrophotometer and KBr pellets. The liquid crystalline phases were identified by optical microscopy using a Nikon polarizing microscope equipped with a Mettler hot stage. The transition temperatures of the materials were determined by using a Perkin-Elmer DSC-7 differential scanning calorimeter (scan rate 5 °C min⁻¹). Analytical TLC was conducted on Whatman precoated silica gel 60-F254 plates.

The induced tilt angle in the chiral smectic A phase was determined by monitoring the intensity changes on the application of an ac electric field.⁹ The polarization measurements were performed via the conventional triangular wave method.¹⁰ Switching time measurements were carried out by monitoring the optical response to a bipolar square wave. The sample cell was secured in a Mettler heating stage and the temperature was elevated to a few degrees above the SmA-isotropic transition of the material. The sample was slowly cooled at a rate of 0.1 °C min⁻¹ into the chiral smectic A phase in presence of a 10 Hz 5 V μm⁻¹ electric field to attain a nearly uniform bookshelf texture. All measurements were performed under a Nikon polarization microscope so that the quality of alignment could be monitored continuously throughout the measurements.

Synthesis. Typical preparations of the new materials are described below.

4'-Hydroxy-4-biphenyl Benzoate (2). To a solution of biphenol 1 (10 g, 80 mmol) in 100 mL of pyridine was added benzoyl chloride (12.65 g, 90 mmol) dropwise over 30 min. The reaction mixture was stirred overnight at room temperature. Water was added and the mixture was stirred for another 30 min. The precipitate was filtered and washed several times with water. The resulting crude white solid was purified by column chromatography on silica gel (eluent: dichloromethane) to give 4'-hydroxy-4-biphenyl benzoate as a white solid in 28% yield. *R*_f 0.24 (dichloromethane). ¹H NMR (acetone-*d*₆, TMS) δ (ppm) 7.25 (d, 2H, ArH); 7.32 (d, 2H, ArH); 7.48–7.78 (m, 7H, ArH); 8.2 (dd, 2H, ArH), 8.4 (s, 1H, HO-Ar). Anal. Calcd for C₁₉H₁₄O₃: C, 78.62; H, 4.83. Found: C, 79.0; H, 4.75.

4'-Hydroxy-3'-nitro-4-biphenyl Benzoate (3). A stirred suspension of 2 (4.3 g, 14.8 mmol) in acetic acid (90 mL) was kept at 15 °C for 10 min. HNO₃ (3.2 mL, *d* = 1.41) was slowly added dropwise over 20 min. The reaction mixture was stirred for another 30 min and then poured in 300 mL of water. After stirring for 20 min, the yellow precipitate was filtered and washed several times with water. Crystallization from a mixture of ethanol/acetic acid afforded 3 as a yellow solid in 84% yield. Mp 162 °C; *R*_f 0.4 (hexane/ethyl acetate 80/20). ¹H NMR (CDCl₃, TMS) δ (ppm) 7.22 (d, 1H, ArH); 7.3 (d, 2H, ArH); 7.48 to 7.74 (m, 5H, ArH); 7.82 (dd, 1H, ArH); 8.22 (d, 2H, ArH); 8.3 (d, 1H, ArH); 10.1 (s, 1H, HO-Ar). Anal. Calcd for C₁₉H₁₃NO₅: C, 68.06; H, 3.9; N, 4.18. Found: C, 68.15; H, 3.82; N, 4.02.

4'-((R)-1-Methylhexyloxy)-3'-nitro-4-biphenylbenzoate (4). To a nitrogen flushed flask containing a mixture of (*S*)-2-heptanol (0.69 g, 5.97 mmol), nitro derivative 3 (2 g, 5.97 mmol), and triphenylphosphine (1.59 g, 6.10 mmol) in 30 mL of dry THF, a solution of diethyl azocarboxylate (0.97 mL, 6.2 mmol) in 10 mL of THF was added dropwise. The reaction mixture was stirred under nitrogen at room temperature overnight. After evaporation of the solvent, the residue was subjected to column chromatography on silica gel (eluent: hexane/ethyl acetate 85/15) to give 4 in 77% yield as yellow liquid. *R*_f 0.4 (hexane/ethyl acetate 85/15). ¹H NMR (CDCl₃, TMS) δ (ppm) 0.9 (t, 3H, CHCH₃); 1.22 to 1.52 (m, 6H, -(CH₂)₃CH₃); 1.35 (d, 3H, CHCH₃); 1.62 (m, 1H, -CH₂(CH₂)₃-); 1.8 (m, 1H, -CH₂(CH₂)₃-); 4.54 (m, 1H, CHCH₃); 7.08 (d, 1H, ArH); 7.26 (d, 2H, ArH); 7.44–7.64 (m, 5H, ArH); 7.67 (dd, 1H, ArH); 7.99 (d,

1H, ArH); 8.19 (dd, 2H, ArH). Anal. Calcd for C₂₆H₂₇NO₅: C, 72.05; H, 6.23; N, 3.23. Found: C, 72.1; H, 6.15; N, 3.2.

4'-((R)-1-Methylhexyloxy)-3'-nitro-4-hydroxybiphenyl (5). To a solution of nitro ether derivative 4 (2 g, 4.62 mmol) in 50 mL of methanol and 15 mL of water, was added LiOH·H₂O (0.86 g, 20.6 mmol). The reaction mixture was stirred overnight at room temperature. After evaporation of the solvent, the residue was neutralized by HCl in ice, and the product was extracted several times with ethyl ether. The combined organic extracts were dried over anhydrous MgSO₄ and evaporated under reduced pressure. The final product was purified by column chromatography on silica gel (eluent: hexane/ethyl acetate 80/20) to give 5 in 97% yield as an orange-red oil. *R*_f 0.2 (eluent: hexane/ethyl acetate 80/20). ¹H NMR (CDCl₃, TMS) δ (ppm) 0.91 (t, 3H, -CH₂CH₃); 1.2–1.56 (m, 6H, -(CH₂)₃CH₃); 1.3 (d, 3H, -CHCH₃); 1.6 (m, 1H, -CH₂(CH₂)₃-); 1.82 (m, 1H, -CH₂(CH₂)₃-); 4.45 (m, 1H, CHCH₃); 6.4 (br s, 1H, -OH); 6.92 (d, 2H, ArH); 7.15 (d, 1H, ArH); 7.38 (d, 2H, ArH); 7.64 (dd, 1H, ArH); 7.95 (d, 1H, ArH). Anal. Calcd for C₁₉H₂₃NO₄: C, 69.3; H, 7.0; N, 4.25. Found: C, 69.2; H, 7.1; N, 4.24.

4'-(9-Decenyloxy)biphenyl-4-carboxylic Acid Methyl Ester (6). To a nitrogen-flushed flask, kept at 0 °C, were added (960 mg, 40 mmol) of oil-free sodium hydride, 7 g (30 mmol) of methyl 4-hydroxyphenylbenzoate, and 150 mL of dry DMF. A solution of (6.57 g, 30 mmol) of 10-bromo-1-decene in 20 mL of DMF was added dropwise to the suspension. The resulting mixture was allowed to stir for 1 h at room temperature and 8 h at 80 °C. The solvent was removed by rotary evaporation in vacuo, and excess sodium hydride was quenched by addition of water. HCl solution (1 N) was poured into the mixture, and the resulting precipitate was filtered and washed with 10% aqueous sodium bicarbonate solution and water. The crude product was recrystallized twice from ethanol to afford 8.7 g (79%) of 6. ¹H NMR (CDCl₃, TMS) δ (ppm): 1.2–2.08 (m, 14H, (CH₂)₉), 3.98 (t, 2H, CH₂O), 4.02 (s, 3H, OCH₃), 5.02 (m, 2H, CH=CH₂), 5.80 (m, 1H, CH=CH₂), 6.95–8.1 (m, 8H, ArH). Anal. Calcd for C₂₄H₃₀O₃: C, 78.68; H, 8.19. Found: C, 78.54; H, 8.08.

4'-(9-Decenyloxy)biphenyl-4-carboxylic acid (7). was obtained by a hydrolysis of the ester derivative in the presence of KOH/ethanol.¹⁰ The crude product was recrystallized from acetic acid to yield 90% of 7. ¹H NMR (DMSO, TMS) δ (ppm) 1.18–2.1 (m, 14H, (CH₂)₉), 3.96 (t, 2H, CH₂O), 5.02 (m, 2H, CH=CH₂), 5.75 (m, 1H, CH=CH₂), 6.98 to 8.15 (m, 8H, ArH). Anal. Calcd for C₂₃H₂₈O₃: C, 78.40; H, 7.95. Found: C, 78.80; H, 7.75.

4-[3'-Nitro-4'-((R)-1-methylhexyloxy)phenyl]phenyl 4-(5-Hexenyloxy)benzoate (8). To a mixture of 4'-(5-hexenyloxy)phenyl-4-carboxylic acid 7 (1 g, 4.54 mmol), the phenol derivative 5 (1.49 g, 4.54 mmol), and DMAP (46.7 mg, 0.37 mmol) in 80 mL of dichloromethane was added 1-(3-(dimethylamino)propyl)-3-ethylcarbodiimide methiodine (EDC·CH₃I, 1.81 g, 6.11 mmol). The mixture was stirred for 24 h at room temperature. After dilution with dichloromethane, the organic phase was washed with water, a saturated solution of sodium bicarbonate, brine, and finally dried over sodium sulfate. The solvent was evaporated, and the residue was purified by column chromatography on silica gel (eluent: hexane/ethyl acetate 85/15) to give 8 in 75% yield. Mp 46 °C; *R*_f 0.8 (hexane/ethyl acetate 85/15). ¹H NMR (CDCl₃, TMS) δ (ppm) 0.89 (t, 3H, -CH₂CH₃); 1.2–1.56 (m, 12H); 1.31 (d, 3H, -CHCH₃); 1.6 (m, 1H, -CH₂(CH₂)₃-); 1.82 (m, 1H, -CH₂(CH₂)₃-); 4.0 (t, 2H, -CH₂OAr); 4.48 (m, 1H, CHCH₃); 4.98 (m, 2H, CH₂=CH-); 5.9 (m, 1H, CH₂=CH-); 6.92 (d, 2H, ArH); 7.1 (d, 1H, ArH); 7.25 (d, 2H, ArH); 7.56 (d, 2H, ArH); 7.65 (dd, 1H, ArH); 8.0 (d, 1H, ArH). Anal. Calcd for C₃₂H₃₇NO₆: C, 72.28; H, 6.96; N, 2.63. Found: C, 72.45; H, 7.01; N, 2.66.

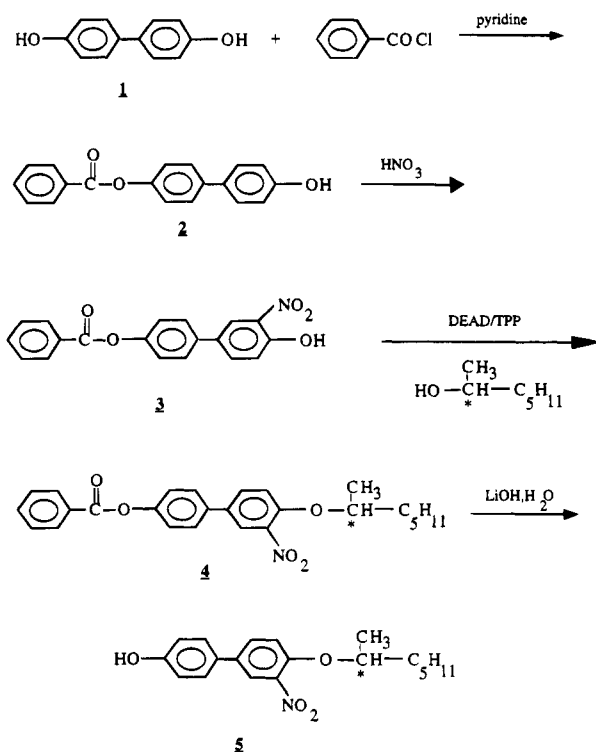
4-[3'-Nitro-4'-((R)-1-methylhexyloxy)phenyl]phenyl 4-(6-Hep-tylmethyltrisiloxyhexyloxy) Benzoate (TSiKN65). The synthesis of the ferroelectric liquid-crystalline material TSiKN65 is given here as an example. The two other materials DSiKN65 and SiKN65 were made following the same procedure. To a solution of heptamethyltrisiloxane (0.4 g, 1.8 mmol) and (0.62

(9) (a) Qiu, R.; Ho, J. T.; Hark, S. K. *Phys. Rev. A* **1988**, *38*, 1653. (b) Lee, S. D.; Patel, J. S. *Appl. Phys. Lett.* **1989**, *54*, 1653.

(10) Miyasato, K.; Abe, S.; Takezoe, H.; Fukuda, A.; Kuze, E. *Jpn. J. Appl. Phys.* **1983**, *22*, L661.

(11) Chan, L. K. M.; Gray, G. W.; Lacey, D.; Scrowston, R. M.; Shenouda, I. G.; Toyne, K. J. *Mol. Cryst. Liq. Cryst.* **1989**, *172*, 125.

Scheme 1



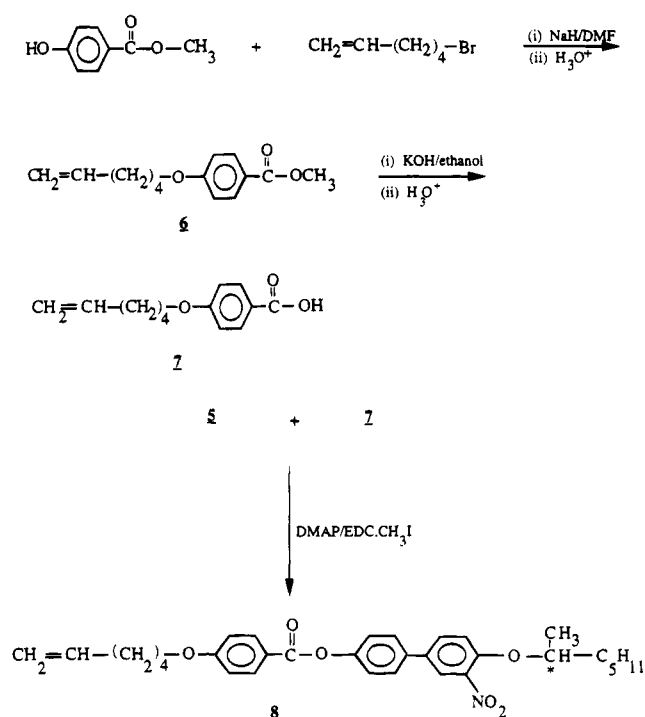
g, 1.16 mmol) of **8**, dissolved in 30 mL of dry THF, were added 5 mg of dicyclopentadienylplatinum(II) chloride catalyst. The reaction mixture was stirred at 60 °C under nitrogen for 24 h. The solvent was removed, and the crude product was purified by column chromatography on silica gel (eluent: hexane/ethyl acetate 90/10). The product was further purified by two crystallizations in ethanol to give **TSiKN65** in 70% yield. R_f 0.4 (hexane/ethyl acetate 90/10). $^1\text{H NMR}$ (CDCl_3) δ (ppm) 0.02 (s, 21H, $\text{Si}(\text{CH}_3)_3$); 0.5 (m, 2H, SiCH_2); 0.88 (t, 3H, $-\text{CH}_2\text{CH}_3$); 1.2–1.54 (m, 14H); 1.31 (d, 3H, $-\text{CHCH}_3$); 1.58 (m, 1H, $-\text{CH}_2(\text{CH}_2)_3-$); 1.8 (m, 1H, $-\text{CH}_2(\text{CH}_2)_3-$); 4.0 (t, 2H, $-\text{CH}_2\text{OAr}$); 4.49 (m, 1H, CHCH_3); 6.93 (d, 2H, ArH); 7.1 (d, 1H, ArH); 7.26 (d, 2H, ArH); 7.56 (d, 2H, ArH); 7.65 (dd, 1H, ArH); 8.15 (d, 1H, ArH). Anal. Calcd for $\text{C}_{39}\text{H}_{59}\text{NO}_8\text{Si}_3$: C, 67.14; H, 8.46; N, 2.0. Found: C, 67.4; H, 8.6; N, 2.1.

Results and Discussion

Synthesis. The synthesis steps leading to the preparation of the chiral liquid crystalline compounds having siloxy end tail groups are illustrated in Schemes 1–3.

The monobenzoyl ester **2** was prepared by reacting biphenol **1** with benzoyl chloride in pyridine. The phenol ring of compound **2** was then selectively nitrated using nitric acid in acetic acid. Nitrophenol **3** was then coupled with (*R*)-2-heptanol using the stereospecific Mitsunobu coupling procedure¹² to give compound **4**. Deprotection of the phenol by hydrolysis of the benzoate ester with hydroxide ion then gave compound **5**. The carboxylic acid derivative **7** was prepared by reacting hydroxybiphenyl carboxylic methyl ester¹³ with 6-bromo-1-hexene in the presence of NaH, followed by hydrolysis. The vinylic derivative material **8** was obtained by esterification of the carboxylic acid derivative **7** with **5** in the presence of 1-(3-(dimethylamino)propyl)-3-ethylcarbodiimide methiodine ($\text{EDC}\cdot\text{CH}_3\text{I}$) and (dimethylami-

Scheme 2



Scheme 3

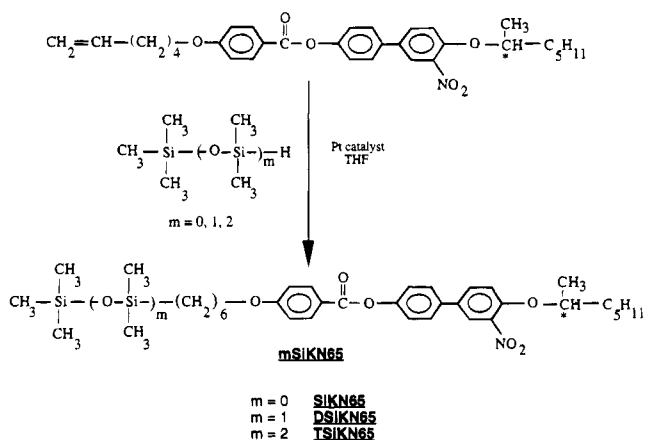


Table 1. Transition Temperatures for the Ferroelectric Organosiloxane Liquid-Crystalline Series

compound	phase sequence (°C) ^a
SiKN65	SmC* 48.2 SmA 51 I
DSiKN65	SmC* 40.5 SmA 55 I
TSiKN65	SmC* 23 SmA 55.5 I

^a For all samples the melting point is below 5 °C.

no)pyridine (DMAP).¹⁴ The corresponding siloxy liquid-crystalline materials were obtained through the classical hydrosilylation reaction¹⁵ between the vinyl mesogenic groups and hydrosiloxane derivatives in the presence of a Pt-catalyst (Scheme 3).

Mesophase Behavior. Phase identification was carried out by means of optical microscopy, the corresponding optical textures being easily identifiable for each mesophase. The transition temperatures as determined by means of DSC (heating runs) are shown in

(12) Mitsunobu, O. *Synthesis* **1981**, 1.

(13) (a) Gray, G. W.; Hartley, J. B.; Jones, B. *J. Chem. Soc.* **1955**, 1412. (b) Marvel, C. S.; Garrison, W. E. *J. Am. Chem. Soc.* **1959**, 4737.

(14) Tschierske, C.; Zschke, H. *J. F. Prakt. Chem.* **1989**, 331, 365.
 (15) Apfel, M. A.; Finkelmann, H.; Janini, G. M.; Laub, R. J.; Luhman, B. H.; Price, A.; Roberts, W. L.; Shaw, T. J.; Smith, C. A. *Anal. Chem.* **1985**, 57, 651.

Table 1. The SmA-isotropic transition of all materials remains practically the same, and the melting points are very low: DSC thermograms show no melting peaks above 5 °C, and the samples kept at room temperature for several months showed no evidence of crystallinity. This lack of crystallinity seems to be associated with the flexibility of the siloxane chains. A number of materials which are the alkyl homologues of these new organosiloxane series **XSikn65** have been studied before.^{1-4,16} All these materials have melting temperatures above room temperatures. We find that the addition of even a single silane unit appears to drastically reduce the melting temperature. We illustrate this point by comparing **SiKN65** with its alkyl analogues **DKN85**¹⁷ and **KN86**¹⁸ (see Scheme 4). All materials have the same number of atoms on the nonchiral chain (eight atoms). **DKN85** has a vinyl group instead of a siloxy unit, at the end of the chain.

The melting points of **DKN85** and **KN86** are 27.5 and 58.9 °C, respectively. Thus, the presence of a single silane unit appears to depress the melting point by more than 25 °C in the case of **DKN85** and more than 55 °C in the case of **KN86**. It is also interesting to note that the presence of a single silane unit induces a smectic C* phase in the material (see Scheme 4). However, increasing the number of siloxy units appears to restabilize the SmA phase by reducing the SmA-SmC* transition temperature (Table 1).

Physical Studies. We will start by presenting the data for the chiral smectic A phase. The chiral smectic A phase exhibits an electroclinic effect as described by Garoff and Meyer.¹⁹ While the phenomenological model to describe the electroclinic effect in the chiral smectic A phase is well established,^{19,20} it is worthwhile to review its predictions here before proceeding with the results and discussion. In the small tilt angle approximation, the tilt angle is predicted to be

$$\theta = \frac{cE}{\alpha_0(T - T_{AC^*})} \quad (1)$$

where c is the electroclinic coupling constant, α_0 is a phenomenological constant, and T_{AC^*} is the SmA-SmC* transition. Equation 1 predicts that θ is linear in E , consistent with experimental observations.²¹ At higher electric field strengths (i.e., larger tilt angles) the tilt angle exhibits a $E^{1/3}$ dependence.⁹ A measure of the electroclinic coefficient c is simply the derivative of eq 1, $d\theta/dE = c/a(T - T_{AC^*})$, or the slope of the θ versus E data. The characteristic time constant is given by

$$\tau = \eta_\theta/a(T - T_C) \quad (2)$$

where η_θ is the rotational viscosity associated with the θ motion. τ is independent of E in the small angle-approximation and has a slight electric field dependence for larger θ .²⁰

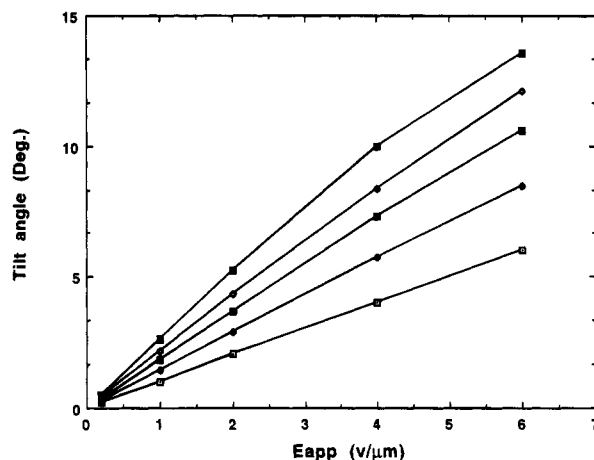


Figure 1. Induced tilt angle for **TSikn65** in the chiral smectic A phase as function of electric field at several temperatures: (■) 25 °C, (◇) 27 °C, (□) 29 °C, (◆) 32 °C, and (□) 34 °C.

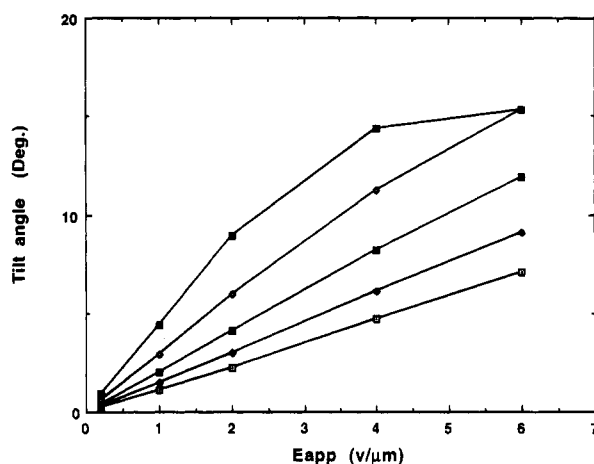
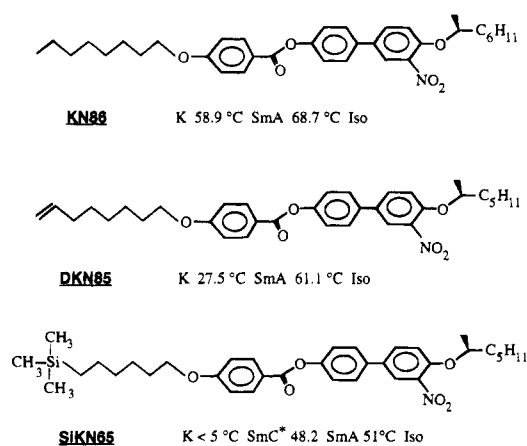


Figure 2. Induced tilt angle for **DSikn65** in the chiral smectic A phase as function of electric field at several temperatures: (■) 43 °C, (◇) 45 °C, (□) 47 °C, (◆) 49 °C, and (□) 51 °C.

Scheme 4



We have measured the induced tilt angle in the chiral smectic A phase as a function of electric field at several temperatures for the **TSikn65** and **DSikn65** materials. We did not perform such measurements on the **SiKN65** material because of the somewhat narrow chiral smectic A temperature range. Figures 1 and 2 show data on the dependence of the electroclinic tilt angle on the applied electric field (E_{app}) for **TSikn65**

(16) Williams, P. A.; Clark, N. A.; Ros, M. B.; Walba, D. M.; Wand, M. D. *Ferroelectrics* **121**, 143, 1991.

(17) Crawford, G. P.; Naciri, J.; Shashidhar, R.; Ratna, B. R. *Mol. Crystals Liq. Cryst.*, in press.

(18) Ratna, B. R.; Crawford, G. P.; Naciri, J.; Shashidhar, R. *SPIE Proceeding: Liquid Crystal Materials, Devices, and Applications III* **1994**, 2175, 79.

(19) Garoff, S.; Meyer, R. B. *Phys. Rev. A* **1979**, *19*, 338.

(20) Abdulhalim, I.; Moddel, G. *Liq. Cryst.* **1991**, *9*, 493.

(21) Davey, A. B.; Crossland, W. A. *Ferroelectrics* **1991**, *114*, 101.

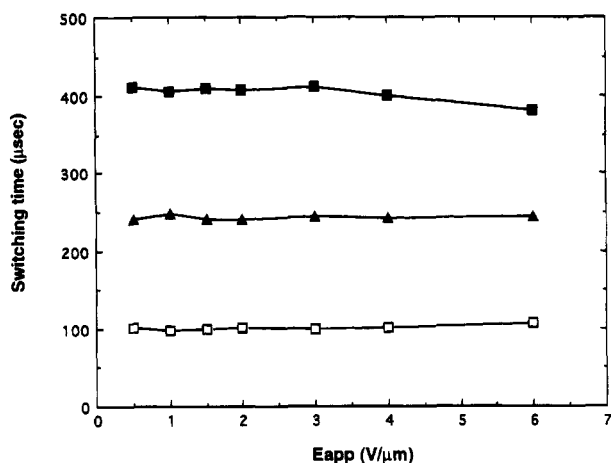


Figure 3. Switching time of **TSiKN65** as a function of electric field at several temperatures: (■) 26 °C, (▲) 28 °C, and (□) 32 °C.

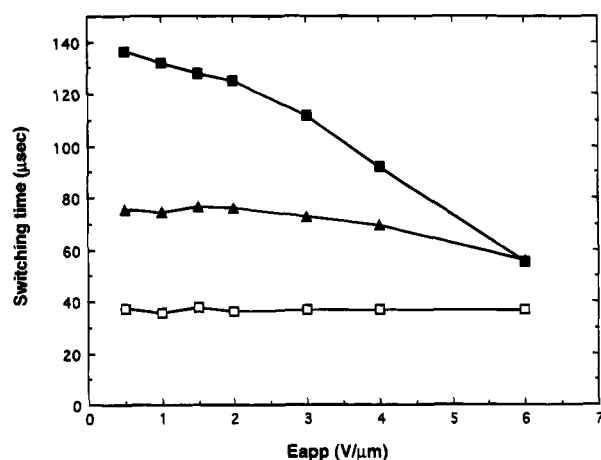


Figure 4. Switching time of **DSiKN65** as a function of electric field at several temperatures: (■) 43 °C, (▲) 45 °C, and (□) 49 °C.

and **DSiKN65**, respectively. Both materials exhibit similar trends except for temperatures very close to the SmA-SmC^* transition. The tilt angle is a linear function of E_{app} for higher temperatures but departs from the linear behavior at lower temperatures. This departure from linearity is more pronounced for **DSiKN65** (Figure 2) than for **TSiKN65** (Figure 1). The tilt angles at the maximum voltage ($6 \text{ V } \mu\text{m}^{-1}$) shown in Figures 1 and 2 are similar for the two materials $\sim 14^\circ$ for **TSiKN65** and $\sim 15^\circ$ for **DSiKN65**. However, there is an important difference; while the tilt angle is saturated for **DSiKN65** at about $6 \text{ V } \mu\text{m}^{-1}$, it still shows an increasing trend for **TSiKN65** at $E_{\text{app}} \sim 6 \text{ V } \mu\text{m}^{-1}$.

Data on the field dependence of the electroclinic switching times (τ) at different temperatures are shown in Figures 3 and 4. For **TSiKN65** (Figure 3), the profile of τ versus E is nearly flat. This field independent behavior of τ is similar to that observed in other electroclinic materials²² at temperatures far from SmA-SmC^* transition. The switching time for **DSiKN65** (Figure 4) also shows a somewhat flat profile, but only away from the SmA-SmC^* transition. At these temperatures τ for **DSiKN65** is substantially less than that

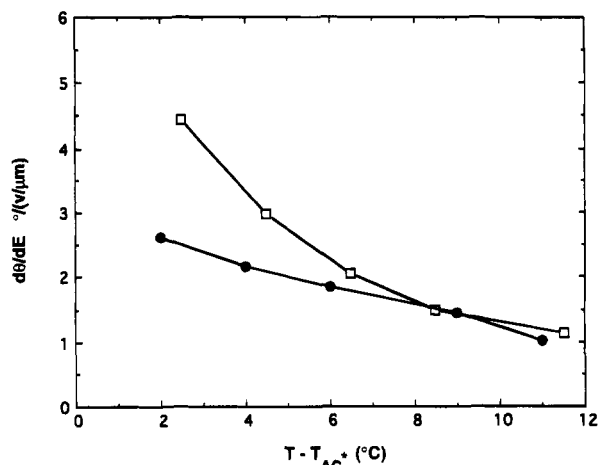


Figure 5. Electroclinic coefficient $d\theta/dE$ of (●) **TSiKN65** and (□) **DSiKN65** at $6 \text{ V } \mu\text{m}^{-1}$, as a function of reduced temperature.

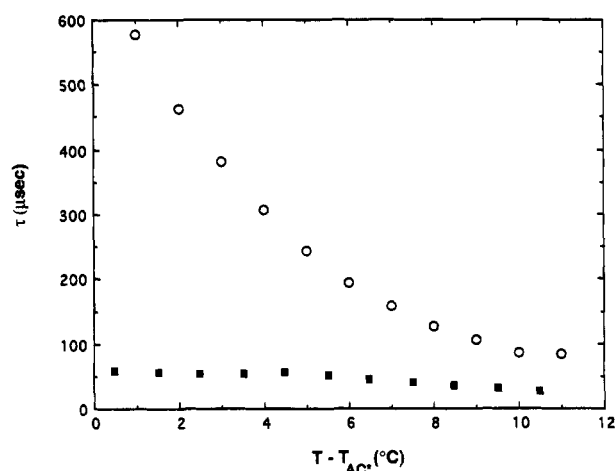


Figure 6. Response time of (■) **DSiKN65** and (○) **TSiKN65** in SmA phase at $6 \text{ V } \mu\text{m}^{-1}$, as a function of reduced temperature.

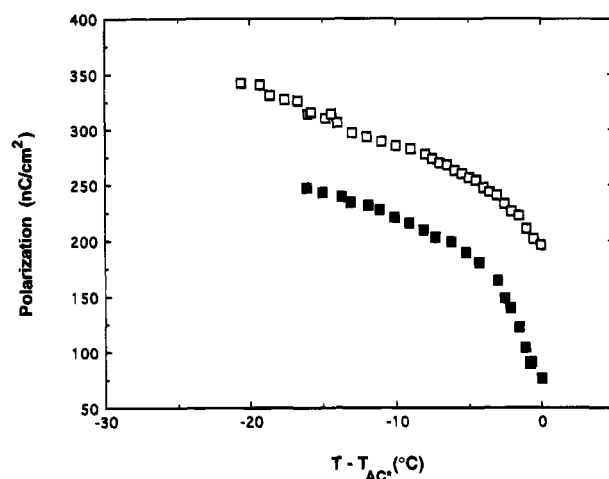


Figure 7. Spontaneous polarization of (■) **DSiKN65** and (□) **SiKN65** in SmC^* phase, as a function of reduced temperature.

for **TSiKN65**. At 43 °C, which is about 2° from the transition, τ exhibits a pronounced dependence on electric field with the response time decreasing with increasing field. This trend, which indicates a departure from the soft-mode like dynamics of the smectic A, could be due to a pronounced tilt order developing close to the SmA-SmC^* transition. Such an increasing trend

(22) Anderson, G.; Dahl, I.; Kuczynski, W.; Lagerwall, S. T.; Skarp, K.; Stebler, B. *Ferroelectrics* **1988**, *84*, 285.

is also predicted by models for materials with large induced tilt angles.²⁰

In Figures 5 and 6, we have plotted the electroclinic coefficient $d\theta/dE$ and the response time (at $6 \text{ V } \mu\text{m}^{-1}$), respectively, as a function of reduced temperature.

According to eqs 1 and 2, both $d\theta/dE$ and τ are expected to show a divergence as the SmA–SmC* transition is approached. It is interesting that while **DSiKN65** shows an increase in the electroclinic coupling on approaching the SmA–SmC* transition, its response time is independent of temperature. On the other hand, **TSiKN65**, which exhibits a weak temperature dependence of $d\theta/dE$, shows a strong critical slowing down of the response time as expected from eq 2. It is important to note here that the response time of **DSiKN65** ($\sim 50 \mu\text{s}$) is much smaller than for the commercially available low molecular mass SCE13 under the same conditions.⁷

We shall now compare the properties of the materials in the SmC* phase. In Figure 7, we have plotted the spontaneous polarization P_s data measured in the SmC* phase of **SiKN65** and **DSiKN65**. We did not measure P_s for **TSiKN65** for which the SmC* exists at subambient temperatures. The polarization of **SiKN65**, in terms of reduced temperature, exhibits one of the highest value of P_s ever reported for similar siloxane materials: 350 nC cm^{-2} at $\sim 20^\circ\text{C}$ below the AC* transition.^{7a} The introduction of an additional siloxy unit in **DSiKN65** reduces the value of P_s . This could be due to the decrease in the effective dipole moment of the molecules, caused by the flexibility of the siloxane chain.⁴ The tilt angle is presented in Figure 8 for the **DSiKN65** and **SiKN65**. Both compounds exhibit a large value of the saturated tilt angle in the SmC* phase which is $\sim 32^\circ$ at 15°C below the AC* transition.

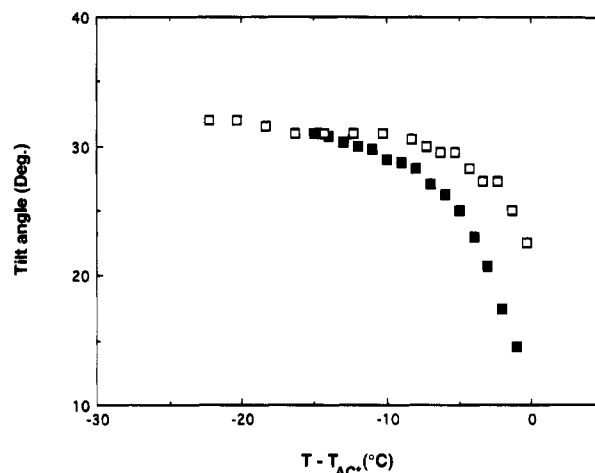


Figure 8. Tilt angle of (■) **DSiKN65** and (□) **SiKN65** in SmC* phase, as a function of reduced temperature.

Summary

We have developed novel electroclinic and ferroelectric liquid crystals containing siloxy chains. The electrooptic properties of these materials is very sensitive to the number of siloxy units attached to the hydrocarbon chain at the nonchiral end of the molecule. These materials exhibit unusually large electroclinic coefficient, even at temperatures well in the smectic A phase. Most importantly, the presence of the siloxy groups decreases the crystallization temperature drastically and maintains low switching times even at ambient temperatures. Currently we are studying the effect of these groups on the chiral end of the molecule.

Acknowledgment. The authors acknowledge the financial support of the Office of Naval Research.

CM950079K